UNIVERSITY OF THESSALY
SCHOOL OF ENGINEERING
DEPARTMENT OF MECHANICAL ENGINEERING

ANALYSIS ON THE FAILURE OF TWIST EXIT ROLLER GUIDES IN STEEL HOT ROLLING

by

CHRIS VASILEIOU

Submitted in partial fulfillment of the requirements for the degree of Diploma in Mechanical Engineering at the University of Thessaly

Volos, 2024

UNIVERSITY OF THESSALY
SCHOOL OF ENGINEERING
DEPARTMENT OF MECHANICAL ENGINEERING

ANALYSIS ON THE FAILURE OF TWIST EXIT ROLLER GUIDES IN STEEL HOT ROLLING

by
CHRIS VASILEIOU

Submitted in partial fulfillment of the requirements for the degree of Diploma in Mechanical Engineering at the University of Thessaly

Volos, 2024

Approved by the Committee on Final Examination:

Advisor — Dr. Emmanouil Bouzakis,
Associate Professor, Department of Mechanical Engineering, University of Thessaly

Member — Dr. Gregory Haidemenopoulos,
Professor, Department of Mechanical Engineering, University of Thessaly

Member — Dr. Alexis Kermanidis,
Associate Professor, Department of Mechanical Engineering, University of Thessaly

Date Approved: [02 29,2024]

Acknowledgements

Θα ήθελα να εκφράσω τις ειλικρινείς ευχαριστίες μου στον επιβλέποντα της διπλωματικής εργασίας μου, Αναπληρωτή Καθηγητή κ. Εμμανουήλ Μπουζάκη, για την πολύτιμη βοήθεια και καθοδήγησή του κατά τη διάρκεια της υλοποίησης της εργασίας μου.

Επίσης, είμαι ευγνώμων στα υπόλοιπα μέλη της εξεταστικής επιτροπής της διπλωματικής εργασίας μου, Καθηγητές κκ. Γρηγόρη Χαϊδεμενόπουλο και Αλέξη Κερμανίδη για την προσεκτική ανάγνωση της εργασίας μου και για τις πολύτιμες υποδείξεις τους.

Ευχαριστώ τους συναδέλφους μου Δημήτρη Κλαρούμενο, Νικόλαο Βλαχοδήμο, Νικόλαο Σταματίου και Βασίλη Νικιφορίδη για την πολύτιμη βοήθειά τους και συνεργασία κατά τη διάρκεια της πρακτικής μου εργασίας στην SOVEL SA. Ευχαριστώ τους φίλους μου Γεώργιο Πλακιά, Φωτεινό Σαμπάνη και Αναστάσιο Κούκουζα για την ηθική υποστήριξή τους.

Τέλος, είμαι ευγνώμων στους γονείς μου, Γεώργιο Βασιλείου και Κατερίνα Λίγγα για την ολόψυχη αγάπη και υποστήριξή τους όλα αυτά τα χρόνια. Αφιερώνω αυτή την εργασία στην μητέρα μου και στον πατέρα μου.

ANALYSIS ON THE FAILURE OF TWIST EXIT ROLLER GUIDES ON HOT ROLLING

CHRIS VASILEIOU

Department of Mechanical Engineering, University of Thessaly

Supervisor: Dr Emmanouil Bouzakis

Associate Professor, Department of Mechanical Engineering, University of Thessaly

Abstract

The objective of this thesis is to conduct a comprehensive examination of the hot rolling process employed in the steel industry. Collaboratively prepared during my internship at SOVEL, a prominent steel manufacturing company specializing in rod bars, this study endeavors to elucidate the fundamental principles of hot rolling. It explores prevalent equipment failures and proposes targeted solutions aimed at mitigating their impact and enhancing overall production efficiency.

Specifically, the thesis scrutinizes the failure patterns observed in twist roller exit guides, critical apparatuses responsible for simultaneously aligning billets and managing torsion. Rolling cylinders, housed within equipment known as rolling mills or stands, serve as pivotal components in this process. Entry and exit guides are strategically positioned at each juncture of the mills to ensure precise billet guidance. Notably, this report focuses on a particular type of exit guide equipped with rollers designed to induce billet torsion.

A primary emphasis is placed on investigating the most common issue associated with these guides: bearing failure within the roller mechanisms. The study meticulously details the hot rolling process from inception to completion, incorporating comprehensive calculations to assess applied forces and conducting fatigue analyses on bearings to ascertain the underlying causes of failure. Furthermore, theoretical solutions are proposed to address these challenges and optimize operational outcomes.

In executing this research, sophisticated software tools such as Autodesk's Inventor 3D Design and Inventor Nastran Professional were leveraged for the development of essential designs and to conduct Finite Element Analysis. This analytical approach served as a critical evaluation technique, facilitating thorough assessments and refinement of final calculations.

Key words: Hot Rolling Process, Steel Industry, Equipment Failures, Bearing Failure

ΑΝΑΛΥΣΗ ΑΣΤΟΧΙΩΝ ΤΩΝ ΟΔΗΓΩΝ ΕΞΟΔΟΥ ΣΤΡΕΨΗΣ ΣΤΗΝ ΘΕΡΜΗ ΕΛΑΣΗ

ΧΡΗΣΤΟΣ ΒΑΣΙΛΕΙΟΥ

Τμήμα Μηχανολόγων Μηχανικών, Πανεπιστήμιο Θεσσαλίας, 2024

Επιβλέπων Καθηγητής: Δρ. Εμμανουήλ Μπουζάκης,

Αναπληρωτής Καθηγητής Κατεργασιών Μορφοποίησης Υλικών

Περίληψη

Ο στόχος αυτής της διπλωματικής εργασίας είναι να πραγματοποιήσει μια σφαιρική εξέταση της διαδικασίας θερμής έλασης που χρησιμοποιείται στη βιομηχανία χάλυβα. Εκπονήθηκε σε συνεργασία κατά τη διάρκεια της πρακτικής μου άσκησης στη SOVEL, μια κορυφαία εταιρεία κατασκευής χάλυβα που εξειδικεύεται στις ράβδους, αυτή η μελέτη επιχειρεί να διασαφηνίσει τις βασικές αρχές της θερμής έλασης. Εξετάζει τις κυριότερες βλάβες εξοπλισμού και προτείνει λύσεις με σκοπό τη μείωση των επιπτώσεών τους και τη βελτίωση της συνολικής απόδοσης παραγωγής.

Ειδικότερα, η παρούσα εργασία εξετάζει τα πρότυπα αποτυχίας που παρατηρούνται στους καθοδηγητές εξόδου των κυλίνδρων περιστροφής, κρίσιμα μέσα που ευθυγραμμίζουν το προϊόν και διαχειρίζονται ταυτόχρονα την στρέψη. Οι κύλινδροι έλασης, που είναι μέρος του εξοπλισμού που ονομάζεται έλαστρο, αποτελούν κρίσιμα κομμάτια σε αυτήν τη διαδικασία. Οδηγοί εισόδου και εξόδου τοποθετούνται στην είσοδο και την έξοδο κάθε ελάστρου για να διασφαλίσουν την ακριβή καθοδήγηση των μεταλλικών προϊόντων. Σημαντικό να σημειωθεί ότι

αυτή η αναφορά επικεντρώνεται σε ένα συγκεκριμένο είδος οδηγών εξόδου εξοπλισμένων με ράουλα που σχεδιάστηκαν για να προκαλούν στρέψη στο προϊόν.

Κύρια εστίαση αποτελεί η διερεύνηση του πιο συνηθισμένου προβλήματος που συνδέεται με αυτούς τους οδηγούς: την αποτυχία των ρουλεμάν εντός των μηχανισμών των ραούλων. Η μελέτη αναλύει λεπτομερώς τη διαδικασία θερμής έλασης από την έναρξη ως την ολοκλήρωση, περιλαμβάνοντας λεπτομερείς υπολογισμούς για την αξιολόγηση των εφαρμοζόμενων δυνάμεων και πραγματοποιώντας αναλύσεις κόπωσης στα ρουλεμάν για να εξεταστούν οι βαθύτερες αιτίες αποτυχίας. Επιπλέον, προτείνονται θεωρητικές λύσεις για την αντιμετώπιση αυτών των αστοχιών και τη βελτιστοποίηση των αποτελεσμάτων λειτουργίας.

Κατά την εκτέλεση αυτής της έρευνας, χρησιμοποιήθηκαν προηγμένα εργαλεία λογισμικού, όπως το Inventor 3D Design της Autodesk και το Inventor Nastran Professional, για την ανάπτυξη των απαραίτητων σχεδίων και τη διεξαγωγή Ανάλυσης Πεπερασμένων Στοιχείων. Αυτή η αναλυτική προσέγγιση χρησιμοποιήθηκε ως κρίσιμη τεχνική αξιολόγησης, διευκολύνοντας λεπτομερείς αξιολογήσεις και βελτιστοποιήσεις των τελικών υπολογισμών.

Λέξεις-κλειδιά: Θερμή Έλαση, Βιομηχανία Χάλυβα, Αστοχία Εξοπλισμού, Αστοχία Ρουλεμάν

Table of Contents

1. Introduction....13

2. Description of the failure 15

3. Analysis on the failure of bearings 22

 3.1 Pitting 22

 3.2 Brinelling 22

 3.3 Cracks 22

 3.4 Scratches 23

4. Failure analysis....25

 4.1 Assembly Process 25

 4.2 Lubrication 27

 4.3 Temperature Variation....28

 4.4 Overloading....29

  4.4.1 Cross-sectional area 29

  4.4.2 Misalignment....31

5. Fatigue Analysis of Ball Bearings....34

6. Assumptions....41

7. Conclusions 42

8. Solution..43

9. References 45

10. Appendix 46

List of Tables

1. Table 5.1: Percentage of Operating Hours of ball bearings based on the deviation of cross-sectional area from guide #1...36
2. Table 5.2: Percentage of Operating Hours of ball bearings based on the deviation of cross-sectional area from guide 1...36
3. Table 5.3: Percentage of Operating Hours of ball bearings based on the deviation of cross-sectional area from guide #1...36
4. Table 5.4: Percentage of Operating Hours of ball bearings based on the misalignment of guide #1 at 900º...37
5. Table 5.5: Percentage of Operating Hours of ball bearings based on the misalignment of guide #2 at 900º...37
6. Table 5.6: Percentage of Operating Hours of ball bearings based on the misalignment of guide #3 at 900º...38
7. Table 5.7: Percentage of Operating Hours of ball bearings based on the misalignment of guide #1 at 1000º 38

8. Table 5.8: Percentage of Operating Hours of ball bearings based on the misalignment of guide #2 at 1000^o 39

9. Table 5.9: Percentage of Operating Hours of ball bearings based on the misalignment of guide #3 at 1000^o 40

1. INTRODUCTION

Hot rolling represents a pivotal metalworking procedure wherein metal is subjected to temperatures surpassing its recrystallization point, facilitating plastic deformation throughout the rolling operation. This method is instrumental in shaping metal into desired geometrical configurations while preserving its original volume. Commencing with the casting process to mold billets into desired shapes and lengths, subsequent steps involve subjecting these billets to furnaces to attain optimal temperatures for proper crystallization. The heated metal then traverses through rolling mills, where rolling cylinders work to flatten, elongate, reduce cross-sectional area, and ensure uniform thickness **[1]**. Predominantly utilized in the metal industry, hot-rolled steel emerges as the prevalent output of this process.

The production of rod-steel bars necessitates a specific processing trajectory within rolling mills. Each pair of rolling mills follows a uniform sequence: the first mill shapes the billet into an elliptical cross-section, succeeded by the second mill which imparts a round cross-section, successively diminishing its diameter until reaching the desired outer diameter. Essential to this process are both horizontal and vertical rolling cylinders as it is mentioned on **[2]** and **[3]**: horizontal cylinders shape the elliptical cross-section, while vertical ones facilitate the formation of a round cross-sectional shape. Subsequently, the billet undergoes cooling and cutting procedures on cooling beds, a process streamlined by the incorporation of shears.

At SOVEL SA, due to outdated equipment, the absence of vertical rolling cylinders necessitates the adaptation of the entire process to rely solely on horizontal cylinders. This adjustment hinges on the presence of specialized equipment capable of precisely twisting the material by 90 degrees after each rolling process, enabling subsequent horizontal cylinders to achieve the desired round cross-sectional shape. However, employing such equipment entails additional operational and maintenance costs attributable to heightened torsional forces exerted on the rollers.

Factors contributing to potential failures of this equipment, that are being pointed out on **[4]**, such as assembly processes, lubrication types and protocols, billet temperature variations and equipment overloading, will be thoroughly examined. Remedial measures will be proposed to either mitigate these risks or prolong intervals between occurrences. Notably, the twist rolling exit guides are sourced and manufactured by an external partner, Danieli, a critical aspect of ensuring operational reliability and efficiency.

2. DESCRIPTION OF THE FAILURE

The issue under scrutiny pertains to recurring problems observed in various twist roller exit guides. A uniform methodology was applied to analyze and calculate the issues across all problematic components. It is noteworthy that such equipment typically does not encounter such frequent failures; ordinarily, maintenance is scheduled based on the gradual wear of rollers due to prolonged exposure to high temperatures from contact with the hot billet as it demonstrated on **[5]** and **[6]**. However, in this instance, the specific exit roller guides were expected to be replaced every twenty days, 240 hours of production, yet failures were occurring as frequently as every two or three days. Consequently, a temporary measure involving the replacement of these guides every two days was implemented as a form of preventative maintenance, pending the identification of a permanent solution.

The failure of the equipment primarily stems from bearing failures, with the larger of the two bearings inside the rollers being the primary point of concern, accounting for approximately 95% of failures. Thus, the investigation focused on this specific type of bearing, supplied by an external partner, SKF, capable of withstanding both radial and axial loads. The bearings are different in size and are not facing each other. Ongoing examinations revealed instances of pitting and brinelling on the inner ring surface, cracks on the outer ring surface, and scratches on the cylindrical roller bearings. While cracks on the outer ring surface were most frequently recorded, various parameters were meticulously examined, including lubrication levels, the condition of associated parts such as spacers and nuts, and potential assembly errors.

An additional aspect warranting thorough examination was the observation that the rollers of the twist exit guides became looser after extended periods of operation, persisting even after scheduled plant shutdowns. This phenomenon may be indicative of incorrect shim placement during the assembly process, a topic to be explored further in Chapter 4. Furthermore, concerns regarding the ingress of external materials into the bearings during operation were raised.

Additionally, excessive accumulation of grease and chips at the base of the guide following daily operations was identified, exacerbating roller rotation difficulties, and contributing to accelerated wear on the guide body. Efforts to address these concerns are integral to ensuring the sustained reliability and performance of the equipment. **Figures 2.1, 2.2, 2.4, 2.6 and 2.7** present detailed views of the twist roller exit guides and **Figures 2.3** and **2.5** from **[7]** their supporting components, intended to provide the reader with a clearer understanding of the equipment in question.

Figure 2.1: Side view of a twist exit roller guide after a production cycle.

Figure 2.2: Front view of various twist exit roller guides from the maintenance workshop.

Figure 2.3: Single row tapered ball SKF bearing used on the twist exit roller guides.

Figure 2.4: Twist exit roller guide assembled on the rolling cylinders just before a production cycle starts.

Figure 2.5: Shims used for eliminating the tolerances during assembly process.

Figure 2.6: The wear observed on the body surface, resulting from contact with the lower roller, can be attributed to the substantial accumulation of grease and chips on the base surface.

Figure 2.7: i) Cracks on the surface of a failed used shaft and ii) cracks which led to the total catastrophic failure of the big sized ball bearing.

3. ANALYSIS ON THE FAILURE OF BEARINGS

3.1 Pitting

Pitting is a phenomenon characterized by the formation of small holes, typically 0.1 mm in depth, on the raceway surface due to rolling fatigue. Common causes include potential reductions in internal clearances during operation, flaws resulting from errors during the mounting process, or inaccuracies in the shapes of shafts or housings. Effective countermeasures often involve upgrading the type of lubricant used and either reducing external loads or switching to a different type of ball bearing. **Figure 3.1** (**[8]**) illustrates this type of failure on the surface of the bearing's inner ring.

3.2 Brinelling

Brinelling refers to depressions formed on the portion of the raceway surface that encounters the rolling element, resulting from plastic deformation. This phenomenon is typically caused by solid external particles or excessively high radial and axial loads. Addressing this type of failure requires a comprehensive investigation to identify the sources of these heavy loads, along with meticulous cleaning during the mounting process. **Figure 3.2** (**[8]**) depicts this form of failure on the inner ring raceway surface of the bearing.

3.3 Cracks

Slight cracks, splitting, and fractures often manifest on the surface of the outer ring. Primary causes typically include overloading, abnormal heat generation, or incorrect installation of the ball bearing. In addition to the countermeasures outlined in Chapter 3.3, solutions aimed at mitigating thermal impacts could also prove effective. **Figure 3.3** (**[8]**) illustrates this type of failure on the outer ring of the bearing.

3.4 Scratches

Scratches are a form of failure resulting from sliding contact, often leading to flaws in the axial direction or cycloidal flaws on the roller end or rib face of the bearing ring that guides rollers. Once more, inadequate lubrication, improper rotation of rolling elements, intrusion of external particles, and overloading are primary causes. Similar countermeasures outlined in Chapters 3.1, 3.2, and 3.3 could effectively address this type of failure. **Figure 3.4** (**[8]**) depicts this form of failure on the outer ring raceway surface of the bearing.

Figure 3.1: Pitting on the inner ring of the bearing.

Figure 3.2: Brinelling observed on the inner ring raceway surface of the bearing.

Figure 3.3: Crack detected on the outer ring of the bearing.

Figure 3.4: Scratch identified on the outer ring raceway surface of the bearing.

4. FAILURE ANALYSIS

4.1 Assembly Process

The initial stage crucial to the entire process is the assembly process, which demands meticulous attention to detail and strict adherence to the manufacturer's instructions. A pristine environment devoid of external contaminants, such as dust, is imperative to ensure the longevity of the equipment's operational life. Each component of the assembly must be mounted with extreme care, avoiding excessive preloads that could lead to catastrophic consequences. Bearings must be mounted according to the precise assembly procedures outlined in SKF handbooks to achieve the necessary clearances for optimal performance. Any deviation from these clearances, whether smaller or larger, can impair the bearing's functionality. Machined parts, such as shims and spacers, must conform to the manufacturer's mechanical specifications, and equipment cooling must be managed according to specified water flow rates.

Over a two-week period, the assembly process for these specific twist exit roller guides underwent rigorous scrutiny and supervision. Every requirement, as mentioned above, was diligently met on each occasion. Additionally, all components utilized were replaced with new ones, cleaned thoroughly with appropriate chemicals, and checked for dimensional accuracy before mounting. Furthermore, technicians involved in these processes adhered to strict criteria regarding attire, ensuring cleanliness and safety with proper attire including clothing, gloves, shoes, glasses, and helmets, all cleaned thoroughly before each use. Moreover, specific tightening torque, as prescribed by ISO standards or the manufacturer, was meticulously applied to every bolt, nut, and component.

During the final three days of this two-week period, an expert technician from the external partner visited the company's workshops to oversee the assembly process. Their feedback was overwhelmingly positive, with only one suggestion regarding the accumulation of grease and waste material on the base surface of the exit roller guide. It was recommended to machine an inclined surface on the equipment's base and install an additional water flow nozzle to facilitate material removal. However, it was noted that this accumulation was not deemed a logical cause for the encountered failures. **Figure 4.1** illustrates the type of wear observed on the outer surface of the twist exit roller guides.

Figure 4.1: Wear observed on the outer surface of the twist exit roller guides.

4.2 Lubrication

The presence of appropriate lubrication is essential for equipment of this nature. It stands as the second most common factor contributing to the reviewed failure, often stemming from the incorrect type or improper application of lubrication. Primarily, lubrication is achieved using grease, which forms a thin layer on the surfaces of moving parts, facilitating smoother movement over one another. Given the multitude of moving and rotating parts in the equipment, the necessity of lubrication is evident.

Regarding the type of lubrication used, namely grease, this choice is in accordance with the manufacturer's recommendations. Moreover, specific grease specifications provided by the manufacturer dictate the type of grease to be used for lubrication. Upon thorough examination, the utilized grease meets all specified requirements across various parameters.

The lubrication process itself requires careful consideration, particularly due to the sensitivity of grease and other lubricants to high temperatures. Prolonged exposure to high temperatures can result in grease melting, leading to the collapse of lubrication films and accelerated abrasion and scuffing of components. Additionally, hot grease can expedite the degradation of filters and seals, accelerating corrosion processes.

To mitigate the effects of melted grease, which is an inevitable consequence of the high temperature of the billet, a specific procedure has been employed. This procedure entails the use of a forced lubrication system that replenishes the required amount of grease at predetermined intervals, allowing for the removal of overheated grease from the equipment. Various intervals for grease replenishment have been tested, yet the reviewed failure persists despite these efforts.

4.3 Temperature Variation

Another crucial parameter requiring examination is the temperature variation exhibited by each billet as it progresses through the production line. Despite meticulous organization and study of the billet heating process in the furnace, minor deviations in the final temperature of each billet are inevitable. These temperature variations can significantly impact the properties of the heated steel, consequently exerting substantial forces on the rollers that may contribute to the occurrence of the initial failure as it can be examined from **[9]** and **[10]**.

To address this concern, specific lower and upper limits for billet temperature needed to be established. By employing equation **6.1** provided by S. Ekelund **[11]**, the lower and upper limits of the billet's yield stress at each temperature can be calculated. This analysis allows for a comprehensive understanding of how temperature fluctuations may influence the mechanical behavior of the billets and their subsequent interaction with the equipment.

$$Kf = (14 - 0.01t)(1.4 + C + Mn + 0.3Cr) \quad kg/mm^2 \quad (\mathbf{4.1})$$

where, t is the temperature to which the steel is heated (above 700^{o}C) in degrees Celsius, C the carbon content of steel on %, Mn the manganese content of steel on % and Cr chromium content of steel on %.

While theoretical values of yield stress provide valuable insights, a decision was made to utilize experimental data obtained from an external partner who conducted relevant tensile and shear tests in accordance with specific standards. In Chapter 5, the impact of temperature will be thoroughly analyzed, shedding light on how variations in temperature affect the operational life of the bearings. This detailed analysis will offer a deeper understanding of the relationship between temperature fluctuations and the performance of the equipment, particularly in relation to the bearings.

4.4 Overloading

4.4.1 Cross-sectional area

One of the pivotal parameters in this study is the torsional forces exerted on the billet. As previously mentioned, the twist exit roller guides have the capability to impart a rotational angle to the billet. Additionally, there are supplementary torsional forces acting on the rollers, necessitating precise calculation. To facilitate this calculation, a fundamental equation from torsion theory is employed.

$$\theta = \frac{TL}{GJ} \ \ radians \quad (\mathbf{4.2})$$

where, θ is the angle of rotation in radians, T the applied torque in Nm, G the shear modulus of the billet in MPa, J the polar moment of inertia from the cross-section area of the billet in mm^4 and L the length of the billet until it reaches the exit guide's rollers in mm.

Angle of rotation in radians is calculated by equation **4.3.**

$$\theta = \left(\frac{x_1}{x_2}\right)\left(\frac{\pi}{2}\right) \ \ radians \quad (\mathbf{4.3})$$

where, x_1 is the distance from the center of rolling cylinders to the center of the next exit guide's rollers in mm and x_2 the distance from the center of rolling cylinders to the center of the next entry guide's rollers in mm.

If the distance x_2 is assumed to be constant, then it follows that the smaller the value of x_1, the lesser the angle of rotation will be. The parameters G, J, and L from equation **4.2** are known based on the properties and dimensional characteristics of the billet. Subsequently, the final value of the applied torque can be calculated.

Moreover, to determine the force applied to each roller, equation **4.4** is utilized. Given that there are two rollers involved in the torsion of the billet, the final value is divided by two to account for this dual contribution.

$$T = Fx \quad Nm \quad \mathbf{(4.4)}$$

where, F is the applied force in N and x the perpendicular distance of the force from the center of rotation in m.

In the specific plant, all values are known and remain constant, including x_1 and x_2, as the manufacturer provides specific designs. The only variable that could affect the calculated forces is the cross-sectional area of the billet. After a billet passes through the rolling cylinders, wear inevitably occurs on the surface of the grooves. While the gap of the grooves is often adjusted to the appropriate size during scheduled plant stops, until this adjustment takes place, a certain type of wear affects the rolling cylinders, resulting in the production of a larger cross-sectional area of the billet. Consequently, the only value that is not always constant in equation **4.2** is the polar moment of inertia J of the billet. In Chapter 5, the effect of this parameter on the operating life of bearings will be elucidated. **Figure 4.2** presents a sketch to better illustrate the billet offset associated with the increase in the polar moment of inertia J.

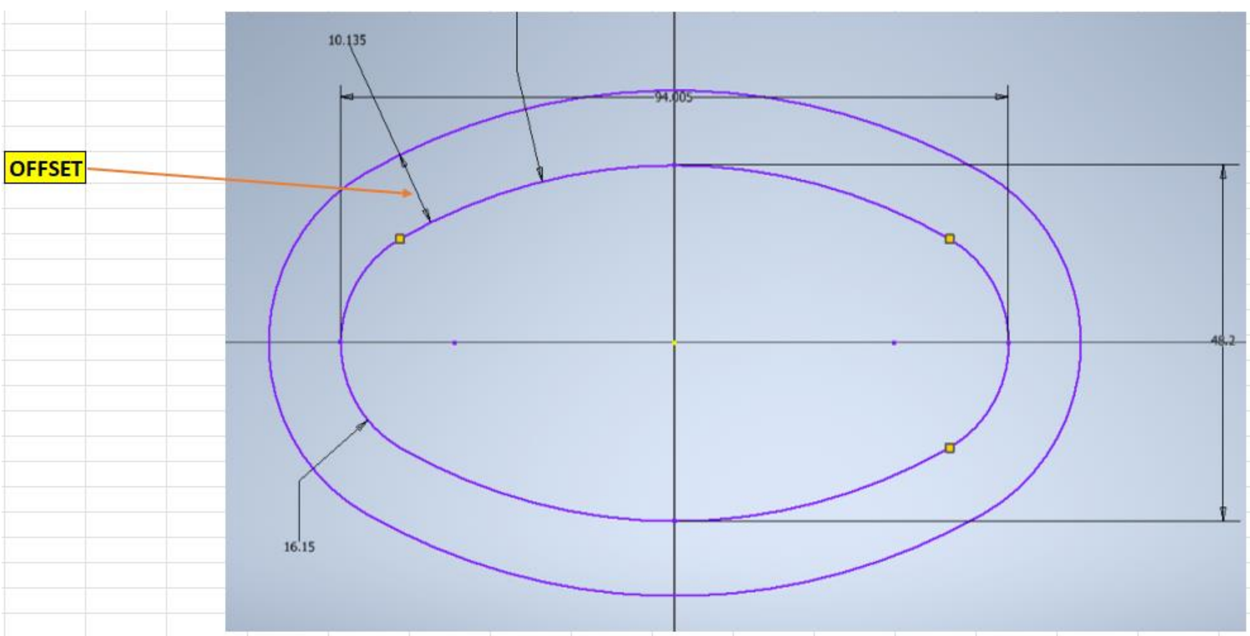

Figure 4.2: The offset of the cross-sectional area is contingent upon the wear of the rolling cylinder's groove.

4.4.2 Misalignment

Arguably, the most critical parameter in this study is the misalignment of the twist exit roller guides relative to the centerline of the rolling cylinders as it is mentioned on **[12]**. Achieving perfect alignment is nearly impossible, and thus, it becomes necessary to calculate this specific phenomenon. Misalignments can occur both axially and vertically.

To better grasp the approach for describing misalignment, it is essential to recall some basic information provided in Chapter 1. After a billet passes through one stand of the rolling mill, it proceeds to the next stand for further processing. For simplicity in calculations, the billet is treated as a beam. Once it reaches the next stand and passes through the rolling cylinders, it behaves like a straight beam with fixed supports at both ends. The billet naturally seeks a perfectly straight path between these stands. Consequently, if there is a slight misalignment in the exit guide, the billet will exert force to align the guide ideally, ensuring the beam remains perfectly straight. This scenario mirrors the bending of a beam. Therefore, it is assumed that when the guide experiences a certain degree of misalignment, the billet applies a force equivalent to that required to bend a beam with fixed ends and produce a displacement equal to the misalignment of the guide. Equation **4.5** is employed to calculate these forces.

$$\delta = (a^3 b^3 F)/(3L^3 EI) \quad mm \quad (\mathbf{4.5})$$

where, δ is the displacement on the point of applied force in mm, a the distance of the force from the left fixed end support in mm, b the distance of the force from the right fixed end support in mm, F the required force in N, L the length of the beam or billet in mm, E the Youngs Modulus of the billet in MPa and I the moment of inertia of the billet in mm^4.

In **Figure 4.3**, the bending phenomenon is depicted. The point of the applied force coincides exactly with where the billet loses contact with the exit guide's rollers. Upon studying Equation

4.5, all values are known except for the moment of inertia. This is due to the elliptical cross-sectional area of the billet, resulting in different values of moment of inertia along the x and y axes. Consequently, if the misalignment occurs along the axial axis, the additional applied force will be considerably larger compared to the phenomenon of vertical misalignment. To gain a clearer understanding of the variance in moment of inertia values along the different axes, Figure **4.4** has been included.

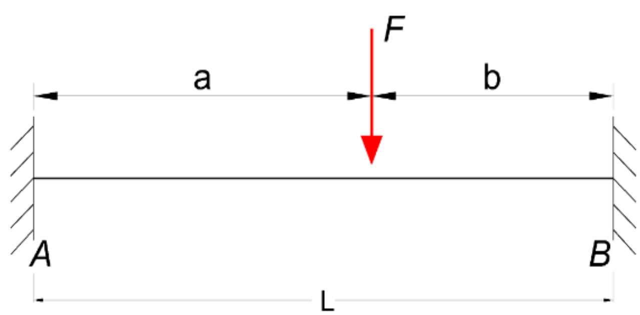

Figure 4.3: The simplification of the bending fixed beam on both ends involves treating the billet as a beam with fixed supports at both ends.

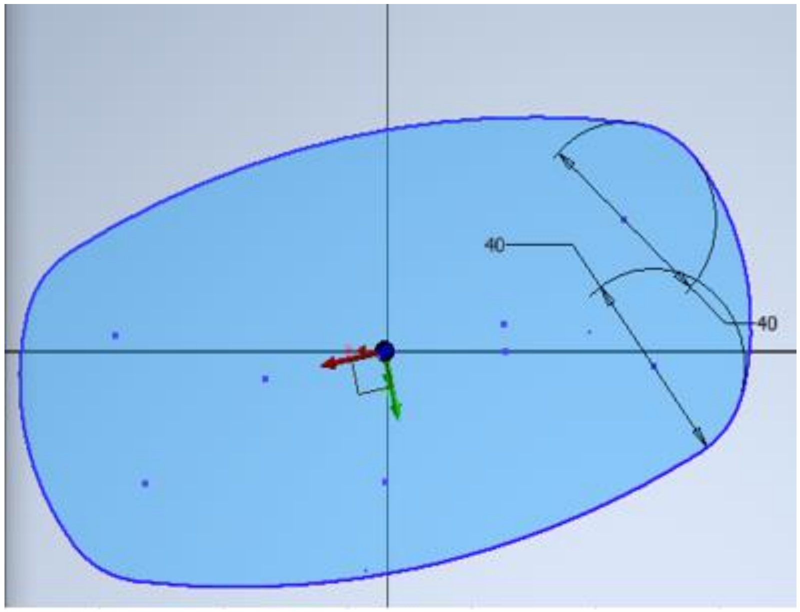

Figure 4.4: The elliptical cross-sectional area of the billet refers to the shape of the billet's cross-section, which resembles an ellipse.

5. FATIGUE ANALYSIS OF BALL BEARINGS

The final phase of the study entails the computation of the operational lifespan of the ball bearings and the evaluation of how various parameters influence this metric.

Primarily, it is imperative to conduct accurate 3D analysis to assess the forces resulting from torsion and misalignment on the roller. Given the bearing's specialized design, capable of withstanding both radial and axial loads, it becomes necessary to analyze the forces as equivalent radial and axial forces acting on the roller's surface. Each roller accommodates two distinct ball bearings of varying sizes. Notably, failures predominantly occurred in the larger bearings, prompting the need for a simplification to appropriately distribute the loads to these bearings. For analytical purposes, it is assumed that the center of each bearing serves as a pinned support, an approach that has been implemented from **[13]**.

Moreover, considering that the point of contact between the billet and the roller consistently lies near the larger bearing, a significant portion of the load is directly transferred to this bearing. This simplification enables the precise calculation of load distribution to each bearing. **Figure 5.1** illustrates the specific assumption made in this regard, where the left and right supports signify the centers of the bearings, albeit with non-actual values provided for illustrative purposes.

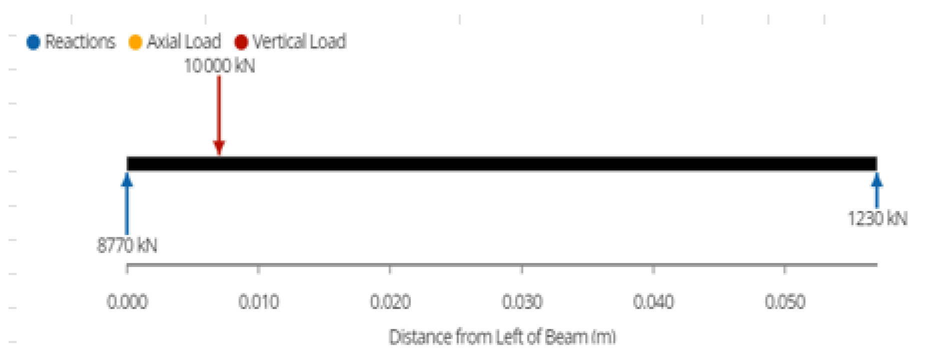

Figure 5.1: A simplification method is employed to facilitate the calculation of load distribution to the bearings.

Subsequently, it is imperative to conduct a comprehensive analysis of the fatigue behavior of the bearings. This analysis relies on vital information compiled from the general catalogue of SKF **[14]** and **[15]**. The ensuing equations were utilized to ascertain the equivalent loads exerted on the bearings.

$$P = F_r, if \quad \frac{F_a}{F_r} < e \quad kN \quad (\mathbf{5.1})$$

$$P = 0.4F_r + YF_a, if \ \frac{F_a}{F_r} > e \quad kN \quad (\mathbf{5.2})$$

$$L_{10} = \left(\frac{C}{P}\right) \quad millions \ revolutions \quad (\mathbf{5.3})$$

$$L_{10h} = \frac{10^6 L_{10}}{60} n \quad hours \quad (\mathbf{5.4})$$

where, C is the basic dynamic load rating in kN, e a calculation factor, Fa the axial load in kN, Fr the radial load in kN, P the equivalent dynamic bearing load in kN, Y a calculation factor, L10 the basic rating life in million revolutions, C the basic dynamic load rating in kN, L10h the basic rating life in operating hours, N the rotational speed in rpm and p an exponent of the life equation depending on the bearing type.

Upon determining the constant factors from the SKF general catalogue, the values of Fa and Fr are computed, leading to the derivation of the L10h value. Parameters such as cross-sectional area and misalignment are integral to these calculations, offering insights into their impact on the bearing's operational lifespan.

In Chapter 4.4, additional radial and axial loads resulting from torsion phenomena are incorporated into the analysis. The subsequent **Tables**, ranging from **5.1 to 5.3**, delineate the percentage impact of each parameter on the bearing's L10h concerning the wear of the rolling cylinder's groove. **Tables 5.4** to **5.9** provide similar insights, but they focus on the effects of axial or vertical misalignment of the equipment. In these tables, the horizontal column represents the axial misalignment value, while the vertical column denotes the vertical misalignment, both measured in millimeters.

Moreover, all calculations outlined in the specified chapter have undergone rigorous validation through multiple finite element analysis simulations. Detailed figures from these simulations can be found in the Appendix.

Offset (mm)	0	0.25	0.5	0.75	1
Percentage on Operating Hours	**100**	**95.9**	**91.6**	**84.5**	**83.7**

Table 5.1: Percentage of Operating Hours of ball bearings based on the deviation of cross-sectional area from guide #1

Offset (mm)	0	0.25	0.5	0.75	1
Percentage on Operating Hours	**100**	**93.9**	**87.8**	**82.1**	**75.6**

Table 5.2: Percentage of Operating Hours of ball bearings based on the deviation of cross-sectional area from guide #2

Offset (mm)	0	0.25	0.5	0.75	1
Percentage on Operating Hours	**100**	**91.2**	**93.8**	**74.1**	**68.1**

Table 5.3: Percentage of Operating Hours of ball bearings based on the deviation of cross-sectional area from guide #3

	δx(mm)	0.00	0.50	1.00	1.50	2.00	2.50	3.00	3.50	4.00	4.50	5.00
δy(mm)												
0.00		100.00	82.98	54.04	22.01	10.86	6.06	3.71	2.38	1.64	1.16	0.84
0.50		81.86	68.64	47.05	19.79	9.96	5.64	3.48	2.26	1.55	1.13	0.81
1.00		67.77	57.40	41.22	17.85	9.15	5.25	3.25	2.16	1.48	1.06	0.77
1.50		56.69	48.40	36.29	16.18	8.44	4.90	3.06	2.03	1.42	1.03	0.74
2.00		47.86	41.19	32.10	14.70	7.80	4.58	2.90	1.93	1.35	0.97	0.74
2.50		40.73	35.29	28.52	13.37	7.22	4.29	2.74	1.84	1.29	0.93	0.71
3.00		34.93	30.45	25.43	12.18	6.67	4.03	2.58	1.74	1.22	0.90	0.68
3.50		30.16	26.43	22.75	11.15	6.22	3.77	2.45	1.68	1.19	0.87	0.64
4.00		26.20	23.07	20.46	10.25	5.77	3.54	2.32	1.58	1.13	0.84	0.61
4.50		22.88	20.27	18.43	9.41	5.38	3.32	2.19	1.51	1.06	0.81	0.61
5.00		20.08	17.89	15.98	8.67	5.00	3.13	2.06	1.45	1.03	0.77	0.58

Table 5.4: Percentage of Operating Hours of ball bearings based on the misalignment of guide #1 at 900^{o}C.

	δx(mm)	0.00	0.50	1.00	1.50	2.00	2.50	3.00	3.50	4.00	4.50	5.00
δy(mm)												
0.00		100.00	81.35	63.59	26.42	13.21	7.46	4.55	2.97	2.02	1.45	1.07
0.50		80.28	66.12	53.92	23.26	11.88	6.83	4.24	2.78	1.90	1.39	1.01
1.00		65.30	54.42	45.76	20.61	10.75	6.26	3.92	2.59	1.83	1.33	0.95
1.50		53.79	45.26	38.43	18.33	9.80	5.75	3.67	2.47	1.71	1.26	0.95
2.00		44.75	38.05	32.55	16.31	8.91	5.31	3.41	2.28	1.64	1.20	0.88
2.50		37.61	32.24	27.81	14.60	8.09	4.93	3.16	2.15	1.52	1.14	0.82
3.00		31.92	27.50	23.89	13.15	7.40	4.55	2.97	2.02	1.45	1.07	0.82
3.50		27.24	23.64	20.67	11.88	6.76	4.24	2.78	1.90	1.39	1.01	0.76
4.00		23.45	20.48	18.02	10.75	6.26	3.92	2.59	1.83	1.33	0.95	0.76
4.50		20.29	17.83	15.74	9.73	5.75	3.67	2.47	1.71	1.26	0.88	0.70
5.00		17.70	15.61	13.84	8.85	5.31	3.41	2.28	1.64	1.20	0.88	0.70

Table 5.5: Percentage of Operating Hours of ball bearings based on the misalignment of guide #2 at 900^{o}C.

	δx(mm)	0.00	0.50	1.00	1.50	2.00	2.50	3.00	3.50	4.00	4.50	5.00
δy(mm)												
0.00		100.00	93.15	86.93	81.20	56.73	35.37	23.38	16.18	11.60	8.60	6.50
0.50		90.67	84.66	79.13	74.07	53.27	33.48	22.26	15.48	11.15	8.28	6.29
1.00		82.45	77.11	72.21	67.70	50.05	31.70	21.22	14.85	10.73	8.00	6.12
1.50		75.15	70.43	66.06	62.04	47.12	30.06	20.24	14.23	10.35	7.72	5.91
2.00		68.68	64.45	60.57	57.01	44.36	28.56	19.33	13.63	9.96	7.44	5.73
2.50		62.92	59.14	55.68	52.46	41.84	27.12	18.46	13.07	9.58	7.20	5.52
3.00		57.78	54.39	51.28	48.37	39.50	25.76	17.65	12.55	9.23	6.96	5.35
3.50		53.16	50.12	47.33	44.70	37.29	24.50	16.88	12.06	8.91	6.71	5.21
4.00		49.00	46.28	43.73	41.38	35.27	23.31	16.15	11.60	8.56	6.50	5.03
4.50		45.26	42.82	40.51	38.38	33.41	22.23	15.45	11.15	8.28	6.29	4.89
5.00		41.91	39.67	37.57	35.65	31.63	21.18	14.82	10.73	7.97	6.08	4.75

Table 5.6: Percentage of Operating Hours of ball bearings based on the misalignment of guide #3 at 900^{o}C.

	δx(mm)	0.00	0.50	1.00	1.50	2.00	2.50	3.00	3.50	4.00	4.50	5.00
δy(mm)												
0.00		100.00	86.35	68.59	31.42	18.21	12.46	9.55	7.97	7.02	6.45	6.07
0.50		85.28	71.12	58.92	28.26	16.88	11.83	9.24	7.78	6.90	6.39	6.01
1.00		70.30	59.42	50.76	25.61	15.75	11.26	8.92	7.59	6.83	6.33	5.95
1.50		58.79	50.26	43.43	23.33	14.80	10.75	8.67	7.47	6.71	6.26	5.95
2.00		49.75	43.05	37.55	21.31	13.91	10.31	8.41	7.28	6.64	6.20	5.88
2.50		42.61	37.24	32.81	19.60	13.09	9.93	8.16	7.15	6.52	6.14	5.82
3.00		36.92	32.50	28.89	18.15	12.40	9.55	7.97	7.02	6.45	6.07	5.82
3.50		32.24	28.64	25.67	16.88	11.76	9.24	7.78	6.90	6.39	6.01	5.76
4.00		28.45	25.48	23.02	15.75	11.26	8.92	7.59	6.83	6.33	5.95	5.76
4.50		25.29	22.83	20.74	14.73	10.75	8.67	7.47	6.71	6.26	5.88	5.70
5.00		22.70	20.61	18.84	13.85	10.31	8.41	7.28	6.64	6.20	5.88	5.70

Table 5.7: Percentage of Operating Hours of ball bearings based on the misalignment of guide #2 at 1000^{o}c.

	δx(mm)	0.00	0.50	1.00	1.50	2.00	2.50	3.00	3.50	4.00	4.50	5.00
δy(mm)												
0.00		100.00	87.98	59.04	27.01	15.86	11.06	8.71	7.38	6.64	6.16	5.84
0.50		86.86	73.64	52.05	24.79	14.96	10.64	8.48	7.26	6.55	6.13	5.81
1.00		72.77	62.40	46.22	22.85	14.15	10.25	8.25	7.16	6.48	6.06	5.77
1.50		61.69	53.40	41.29	21.18	13.44	9.90	8.06	7.03	6.42	6.03	5.74
2.00		52.86	46.19	37.10	19.70	12.80	9.58	7.90	6.93	6.35	5.97	5.74
2.50		45.73	40.29	33.52	18.37	12.22	9.29	7.74	6.84	6.29	5.93	5.71
3.00		39.93	35.45	30.43	17.18	11.67	9.03	7.58	6.74	6.22	5.90	5.68
3.50		35.16	31.43	27.75	16.15	11.22	8.77	7.45	6.68	6.19	5.87	5.64
4.00		31.20	28.07	25.46	15.25	10.77	8.54	7.32	6.58	6.13	5.84	5.61
4.50		27.88	25.27	23.43	14.41	10.38	8.32	7.19	6.51	6.06	5.81	5.61
5.00		25.08	22.89	20.98	13.67	10.00	8.13	7.06	6.45	6.03	5.77	5.58

Table 5.8: Percentage of Operating Hours of ball bearings based on the misalignment of guide #1 at 1000^oC.

	δx(mm)	0.00	0.50	1.00	1.50	2.00	2.50	3.00	3.50	4.00	4.50	5.00
δy(mm)												
0.00		100.00	98.15	91.93	86.20	61.73	40.37	28.38	21.18	16.60	13.60	11.50
0.50		95.67	89.66	84.13	79.07	58.27	38.48	27.26	20.48	16.15	13.28	11.29
1.00		87.45	82.11	77.21	72.70	55.05	36.70	26.22	19.85	15.73	13.00	11.12
1.50		80.15	75.43	71.06	67.04	52.12	35.06	25.24	19.23	15.35	12.72	10.91
2.00		73.68	69.45	65.57	62.01	49.36	33.56	24.33	18.63	14.96	12.44	10.73
2.50		67.92	64.14	60.68	57.46	51.84	32.12	23.46	18.07	14.58	12.20	10.52
3.00		62.78	59.39	56.28	53.37	44.50	30.76	22.65	17.55	14.23	11.96	10.35
3.50		58.16	55.12	52.33	49.70	42.29	29.50	21.88	17.06	13.91	11.71	10.21
4.00		54.00	51.28	48.73	46.38	40.27	28.31	21.15	16.60	13.56	11.50	10.03
4.50		50.26	47.82	45.51	43.38	38.41	27.23	20.45	16.15	13.28	11.29	9.89
5.00		46.91	44.67	42.57	40.65	36.63	26.18	19.82	15.73	12.97	11.08	9.75

Table 5.9: Percentage of Operating Hours of ball bearings based on the misalignment of guide #3 at 1000^{o}C.

6. ASSUMPTIONS

After meticulous analysis of the tables, several noteworthy conclusions emerge. Firstly, the cross-sectional area of the billet exhibits a minimal impact on the operational lifespan of the ball bearing. **Figures 5.2**, **5.3**, and **5.4** illustrate that even with a 1mm offset, the bearing's operational life only diminishes to 70%, a level deemed acceptable. Moreover, such a 1mm offset is rarely observed after the wear of the rolling cylinders, as the daily production duration typically falls short of achieving such a deviation. Given that the offset returns to zero after each production cycle, it is reasonable to assert that this parameter is not the primary cause of failure.

In contrast, the **Tables** pertaining to misalignment parameters (**5.5** through **5.9**) reveal a substantial effect on the ball bearing's operational life. Specifically, axial misalignment exerts a more pronounced impact, which is logical for two reasons. Firstly, the billet's moment of inertia is greater along the axial axis, necessitating higher forces for equivalent displacement. Secondly, axial misalignment introduces an additional equivalent force nearly parallel to the axial axis, resulting in a predominant axial load. Conversely, vertical misalignment transfers the equivalent load to the bearing as a radial force.

Interestingly, the temperature deviation of the billet demonstrates no discernible effect on the operational life of the bearing. If such an effect existed, a more drastic reduction in L10h percentage would be evident in **Tables 5.7-5.9** compared to **Tables 5.4-5.6**.

From an assembly process standpoint, addressing the effective removal of excess grease and debris during operation is crucial, as these factors impede the roller's rotation and consequently impact the structural integrity of the guide's body. Additionally, a more precise method for the placement of shims is warranted. The appropriate number of shims must be determined to achieve the desired rotational stiffness of the roller, striking a balance between too loose and too stiff.

Finally, devising a more effective solution to prevent external material ingress into the bearings is imperative to mitigate potential damage and prolong operational longevity.

7. CONCLUSIONS

In summary, the study report suggests that the primary issue lies in the misalignment of the equipment, with minor adjustments required for other parameters outlined in Chapter 6. Two proposed solutions address the concern of excess grease and chip accumulation. Firstly, a redesigned guide's base with an open structure allows debris to freely drop onto the rest bar surface, supplemented by an additional water supply nozzle for continuous cleaning, as depicted in **Figure 7.1**.

Regarding the measurement of the correct number of shims, a procedure recommended by Danieli technicians involves initial assembly without shims, followed by measurement of axial clearance. Shims are then added as necessary to achieve the desired rotational stiffness of the roller.

Unfortunately, improving protection against external material ingress into the bearings proves challenging, necessitating frequent replacement every two to three days to prevent pitting phenomena. This solution, albeit effective, contradicts company policy due to increased workload.

While bearings capable of withstanding higher loads are available, their application is impractical due to specific roller design constraints identified in a prior study. Consequently, addressing misalignment emerges as the most pertinent solution from both mechanical and technical perspectives.

8. SOLUTION

Despite implementing various solutions and suggestions within the workshop and plant, the problem persists, necessitating the decision to change equipment twice per week. A practical solution for accurate equipment misalignment alignment is required. A potential solution, that is being suggested from **[16]**, involves aligning the rest bar to the pass line center using alignment laser equipment and a steel laminate mounted with M8 bolts. A specially designed steel base supports the alignment laser, projecting intersecting lines onto the rest bar surface for precise axial alignment, as depicted in **Figure 9.2**. Detailed drawings of the concept's components are available in the Appendix, particularly **Figures 9.8-9.11**. However, this solution remains untested in the plant and requires further evaluation.

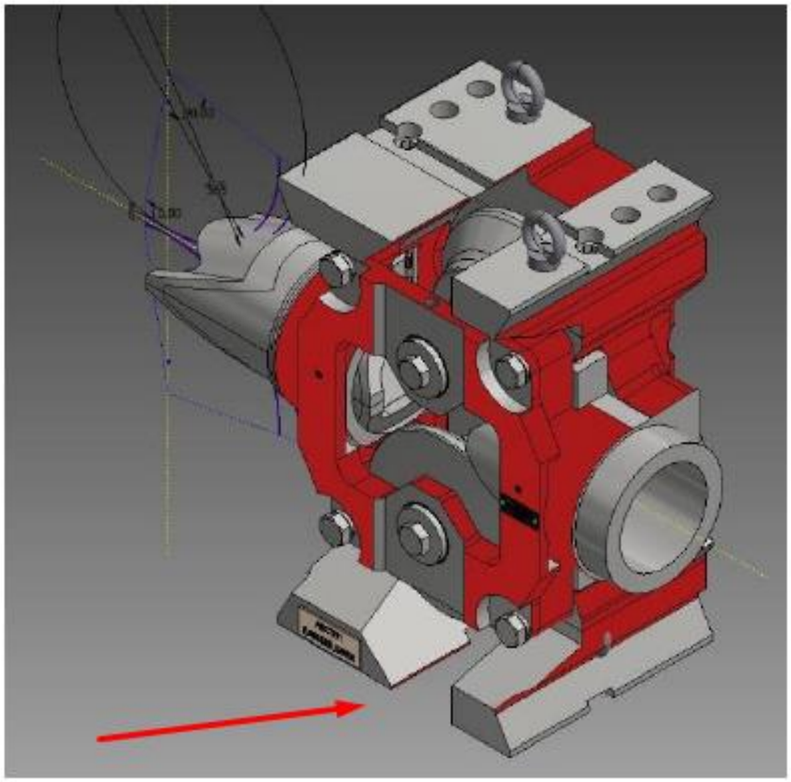

Figure 8.1: Suggested 3D design of a new guide's base

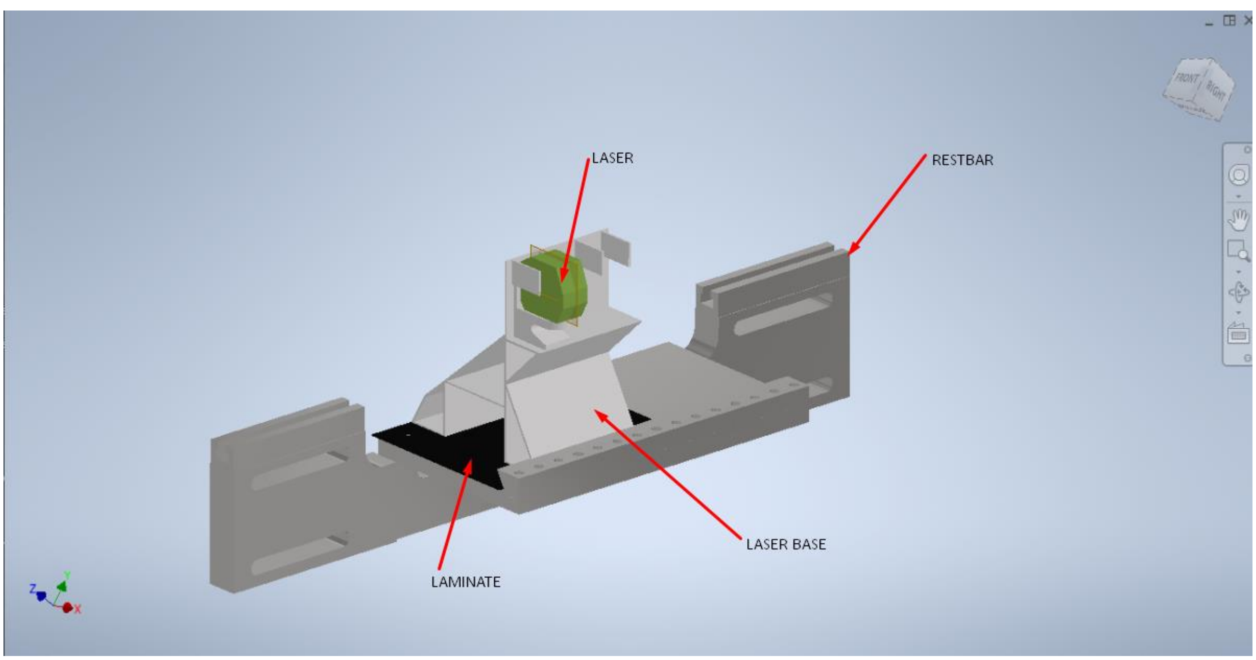

Figure 8.2: 3D Design of alignment laser device for guides.

9. REFERENCES

[1] Jing Limei, (2001) Rolling Mill Roll Design, Durham University.

[2] Xiao Kai Wang, Lin Hua, Chun Dong Zhu, (2011) Optimal Design of the Guide Mechanism on Rolling Mill.

[3] Remn-Min Guo, Optimization Procedure of Rolling Mill Design, New Delhi, India.

[4] Tuukka Tuomi, (2022) Sling Integrated Roller Guide Study, Tempere University.

[5] Bo Wang, (1996) A simulation of roll wear in hot rolling processes, University of Wollongong.

[6] Ben Wright, (2012) Thermal Behaviour of Work Rolls in the Hot Rolling Process, Cardiff University.

[7] V.G.Drozd, P.I.Tetel'baum, I.F.Prikhodko, (1961) Roller Guide equipment for rolling mills.

[8] Koyo (2005) Ball & Roller Bearings, failures, causes and countermeasures by JEKT Corporation.

[9] Jinwoo Lee, (2012) Elevated-Temperature Properties of Steel for Structural Engineering Analysis, University of Texas, Austin.

[10] Chrysanthos Maraveas, Konstantinos Daniel Tsavdaridis, (2017) Mechanical properties of Steel at elevated temperatures before cooling down.

[11] Zygmunt Wusatowski, (2000) Fundamentals of Rolling D.Sc. Professor of the Polytechnical University, Gliwice, Poland.

[12] Lorenzo Soler Blanco, (2020) Roll Alignment in the Steel Industry

[13] Peter Sulka, Milan Sapieta, (2018) Static structural analysis of rolling ball bearing, Department of Applied Mechanics, Faculty of mechanical engineering, University of Zilina, Slovak Republic.

[14] SKF General technical catalogue (2013).

[15] Ms. Shelke, Prof. Galhe D.S., (2016) Fatigue Analysis of Bearing.

[16] Han-Kai Hsu, Jong-Ning Aoh, (2019) The Mechanism of Position-Mode Guide on Correcting Camber in Roughing Process of a Hot Strip Mill.

10. APPENDIX

Data				
α=	14.8	degrees o	0.258178	radians
OA=OB=	80.5	mm or	0.0805	m
OΓ=	77.83197492	mm		
AΓ=	2.668025078	mm		
BΓ=	20.55319147	mm		
J=	28288006	mm4	PERFECT BILLET	
L=	690	mm or	0.69	m
tensile yield stress=	69.3	MPa		
shear yield stress=	40.01037365	Mpa		
p=	65	mm		
γ=	0.024321095			
G (Shear Modulus)=	1645.08932	Mpa or	1.645089	Gpa
T=	17412518.31	Nmm		
2F=	216304.5753	N		
F=	108152.2876	N or	108.1523	kN
J=	31316147	mm4	BAD BILLET	(Not fully correct)
T=	19276472.97	Nmm		
2F=	247667.7868	Nmm		
F=	123833.8934	N or	123.8339	kN
ϕ=	88	degrees o	1.536	radians
x=	108086.8197			
Ffinal=	123908.8993	N or	123.9089	kN

Inputs

Ouputs

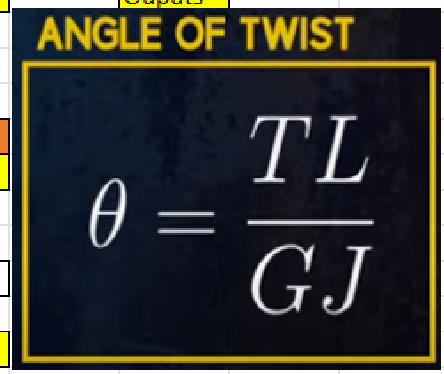

COMMENT: Edit only the required angle of rotation, distance until the required twist angle and the properties of the material and billet in different cass for each exit guide of our production

Figure 10.1: Excel table for the calculation of torsion forces.

x1(mm)	x2(mm)	Contact Patch(mm	Point Load at x(mm	angle a (degree	cos(a)	x distance (mm	sin(a)	y distance (mm)	z distance (mm	φ (radians)	θ (radians)	F (kN)	Fr (kN)	Fa (kN)	
0	4	4	2	35	0.81933	13.36134074	0.573323	136.3533545	40	0.097679	0.285349787	108.17	**107.6543781**	**10.54911**	
1	5	4	3	35	0.81933	12.5420111	0.573323	135.7800318	40	0.092109	0.286489929	108.17	**107.7114665**	**9.949316**	
2	6	4	4	35	0.81933	11.72268147	0.573323	135.2067091	40	0.086486	0.287638966	108.17	**107.7657089**	**9.343494**	
3	7	4	5	35	0.81933	10.90335184	0.573323	134.6333863	40	0.080809	0.288796998	108.17	**107.8170108**	**8.731614**	
4	8	4	6	35	0.81933	10.08402221	0.573323	134.0600636	40	0.075079	0.289964128	108.17	**107.8652755**	**8.113646**	
5	9	4	7	35	0.81933	9.264692578	0.573323	133.4867409	40	0.069294	0.291140461	108.17	**107.9104046**	**7.489558**	
6	10	4	8	35	0.81933	8.445362947	0.573323	132.9134181	40	0.063455	0.292326103	108.17	**107.9522976**	**6.859325**	
7	11	4	9	35	0.81933	7.626033315	0.573323	132.3400954	40	0.057561	0.293521162	108.17	**107.9908522**	**6.22292**	
8	12	4	10	35	0.81933	6.806703683	0.573323	131.7667727	40	0.051611	0.294725745	108.17	**108.0259642**	**5.58032**	
9	13	4	11	35	0.81933	5.987374052	0.573323	131.19345	40	0.045606	0.295939965	108.17	**108.0575272**	**4.931503**	
10	14	4	12	35	0.81933	5.16804442	0.573323	130.6201272	40	0.039545	0.297163934	108.17	**108.0854333**	**4.276449**	
11	15	4	13	35	0.81933	4.348714788	0.573323	130.0468045	40	0.033427	0.298397766	108.17	**108.1095724**	**3.615142**	
12	16	4	14	35	0.81933	3.529385157	0.573323	129.4734818	40	0.027253	0.299641577	108.17	**108.1298328**	**2.947568**	
13	17	4	15	35	0.81933	2.710055525	0.573323	128.900159	40	0.021021	0.300895484	108.17	**108.1461009**	**2.273713**	
14	18	4	16	35	0.81933	1.890725893	0.573323	128.3268363	40	0.014733	0.302159607	108.17	**108.1582611**	**1.593569**	
15	19	4	17	35	0.81933	1.071396262	0.573323	127.7535136	40	0.008386	0.303434067	108.17	**108.1661963**	**0.907129**	
16	20	4	18	35	0.81933	0.25206663	0.573323	127.1801908	40	0.001982	0.304718987	108.17	**108.1697875**	**0.214389**	
17	21	4	19	35	0.81933	0.567263002	0.573323	126.6068681	40	0.00448	0.306014493	108.17	**108.1689143**	**0.484652**	
18	22	4	20	35	0.81933	1.386592633	0.573323	126.0335454	40	0.011001	0.307320711	108.17	**108.1634542**	**1.18999**	
19	23	4	21	35	0.81933	2.205922265	0.573323	125.4602226	40	0.017581	0.308637771	108.17	**108.1532835**	**1.901621**	
20	24	4	22	35	0.81933	3.025251897	0.573323	124.8868999	40	0.024219	0.309965802	108.17	**108.1382769**	**2.619534**	
21	25	4	23	35	0.81933	3.844581528	0.573323	124.3135772	40	0.030917	0.311304938	108.17	**108.1183076**	**3.343719**	
22	26	4	24	35	0.81933	4.66391116	0.573323	123.7402544	40	0.037673	0.312655315	108.17	**108.0932474**	**4.074158**	
23	27	4	25	35	0.81933	5.483240792	0.573323	123.1669317	40	0.044489	0.314017069	108.17	**108.0629669**	**4.810831**	
24	28	4	26	35	0.81933	6.302570423	0.573323	122.593609	40	0.051365	0.315390339	108.17	**108.0273352**	**5.553714**	
25	29	4	27	35	0.81933	7.121900055	0.573323	122.0202862	40	0.0583	0.316775267	108.17	**107.9862207**	**6.30278**	**Perfect point of contact without misalignment!**
26	30	4	28	35	0.81933	7.941229687	0.573323	121.4469635	40	0.065296	0.318171996	108.17	**107.9394904**	**7.057997**	
27	31	4	29	35	0.81933	8.760559319	0.573323	120.8736408	40	0.07235	0.319580674	108.17	**107.8870104**	**7.819327**	
28	32	4	30	35	0.81933	9.57988895	0.573323	120.300318	40	0.079465	0.321001447	108.17	**107.8286463**	**8.586731**	
29	33	4	31	35	0.81933	10.39921858	0.573323	119.7269953	40	0.08664	0.322434466	108.17	**107.7642624**	**9.360162**	
30	34	4	32	35	0.81933	11.21854821	0.573323	119.1536726	40	0.093875	0.323879886	108.17	**107.693723**	**10.13957**	
31	35	4	33	35	0.81933	12.03787785	0.573323	118.5803499	40	0.10117	0.32533786	108.17	**107.6168916**	**10.9249**	
32	36	4	34	35	0.81933	12.85720748	0.573323	118.0070271	40	0.108525	0.326808547	108.17	**107.5336314**	**11.7161**	
33	37	4	35	35	0.81933	13.67653711	0.573323	117.4337044	40	0.115939	0.328292109	108.17	**107.4438055**	**12.5131**	
34	38	4	36	35	0.81933	14.49586674	0.573323	116.8603817	40	0.123414	0.329788707	108.17	**107.3472768**	**13.31582**	
35	39	4	37	35	0.81933	15.31519637	0.573323	116.2870589	40	0.130948	0.331298507	108.17	**107.2439085**	**14.1242**	
36	40	4	38	35	0.81933	16.134526	0.573323	115.7137362	40	0.138542	0.332821679	108.17	**107.133564**	**14.93815**	
37	41	4	39	35	0.81933	16.95385564	0.573323	115.1404135	40	0.146195	0.334358394	108.17	**107.0161072**	**15.75759**	
38	42	4	40	35	0.81933	17.77318527	0.573323	114.5670907	40	0.153907	0.335908824	108.17	**106.8914025**	**16.58243**	
39	43	4	41	35	0.81933	18.5925149	0.573323	113.993768	40	0.161678	0.337473149	108.17	**106.7593153**	**17.41257**	
40	44	4	42	35	0.81933	19.41184453	0.573323	113.4204453	40	0.169507	0.339051546	108.17	**106.6197118**	**18.2479**	

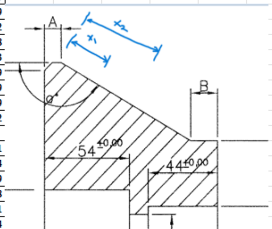

Figure 10.2: Excel table for the calculation of difference on Fa and Fr forces depending the point of contact of the billet and the roller.

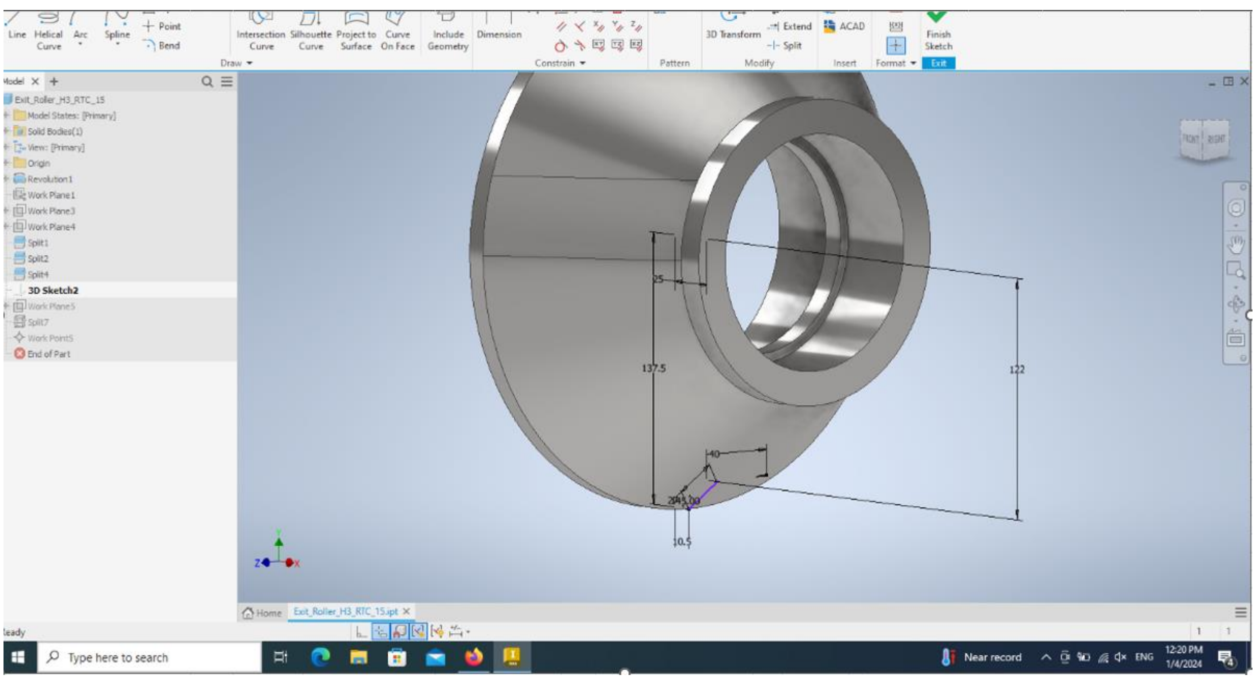

Figure 10.3: 3D design of the roller.

COMMENT:Edit only angles for force analysis from 3D design of the roller and the required Torsion Force			Inputs
			Outputs
Ff=	108.15	kN	
a=	72	degrees	
a=	1.256	radians	
Fxz=	102.84	kN	
Fx=	102.77	kN	
b=	18	degrees	
b=	0.314	radians	
Fyz=	33.404	kN	
Fy=	33.381	kN	
Fr=	**108.05**	**kN**	
extra Fr from misalignment=	0.00	kN	
Frfinal=	**108**	**kN**	
c=	2.12	degrees	
c=	0.037	radians	
Fz or Fa=	3.9987	kN	
extra Fa from misalignment=	0.00	kN	
Fafinal=	**4**	**kN**	
F% to big BB	0.8772	87.7192982	%
F% to small BB	0.1228	12.2807018	%
Frfinal to big BB=	**94.8**	**kN**	
Fafinal to big BB=	**3.51**	**kN**	

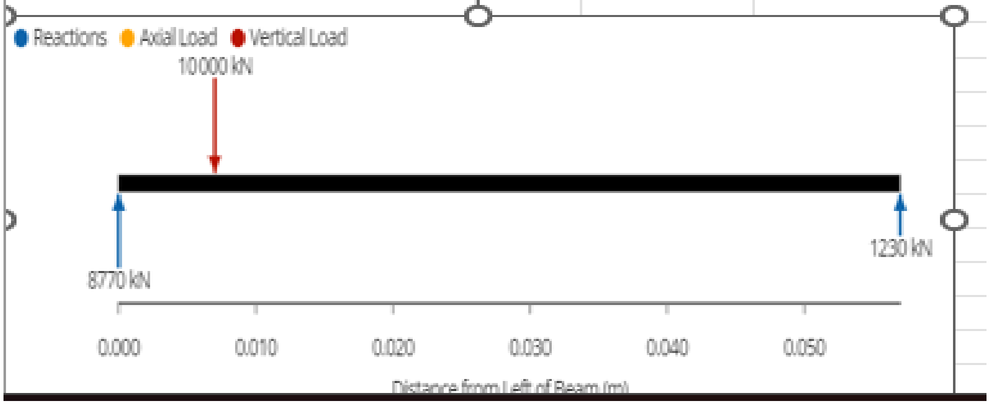

Figure 10.4: Excel table for the proper analyze of external loads and the proper distribution on the bearings.

COMMENT: Nothing to edit. Set parameters and values from SKF about the specific Ball Bearing (32313)

Ball Bearing Data				
e (BB factor)	0.34		Dyn Radial Factor X=	0.4
C (Dyn Load)=	264	kN	Static Radianl Factor X	0.5
Co (Static Load)=	335	kN	Dynamic Axial Factor Y	1.7
Speed n=	177	rpm	Static Axial Factor Y0=	0.9
factor p=	3.333			

Dynamic Load P=	163	kN
ThStatic Load P0=	123	kN
AcStatic Load P0=	128	kN
static SafetyFactor	**2.63**	
dynamic SafetyFactor	**1.62**	
Life in million revs	5.03	
Life on hours	**474**	

COMMENT: Edit only the properties of the beam, its the point where the force is applied and the re **misalignment** of the exit guide from the initial

Vertical Misalignment		
I (moment of inertia)	7454164	mm4
L (Length)=	4400	mm
a=	690	mm
b=	3710	mm
E(Youngs Modulus)=	69.3	GPa (kN/mm2)
δ (displacement)=	**3**	**mm**
F (force)=	23.61	kN
ϕ=	14.8	degrees
ϕ=	0.258177778	radians
Fr=	**22.83**	**kN**
Fa=	**6.03**	**kN**
Frfinal to big BB=	**20.022626**	**kN**
Fafinal to big BB=	**5.287401**	**kN**

Axial Misalignment		
I (moment of inertia)	20833842	mm4
L (Length)=	4200	mm
a=	690	mm
b=	3510	mm
E(Youngs Modulus)=	69.3	GPa (kN/mm2)
δ (displacement)=	**3**	**mm**
F (force)=	67.77	kN
ϕ=	14.8	degrees
ϕ=	0.258177778	radians
Fr=	**17.30**	**kN**
Fa=	**65.52**	**kN**
Frfinal to big BB=	**15.177593**	**kN**
Fafinal to big BB=	**57.475357**	**kN**

Figure 10.5: Excel table for the fatigue analysis of the bearing and the calculation of extra applied forces concerning the axial and vertical misalignment.

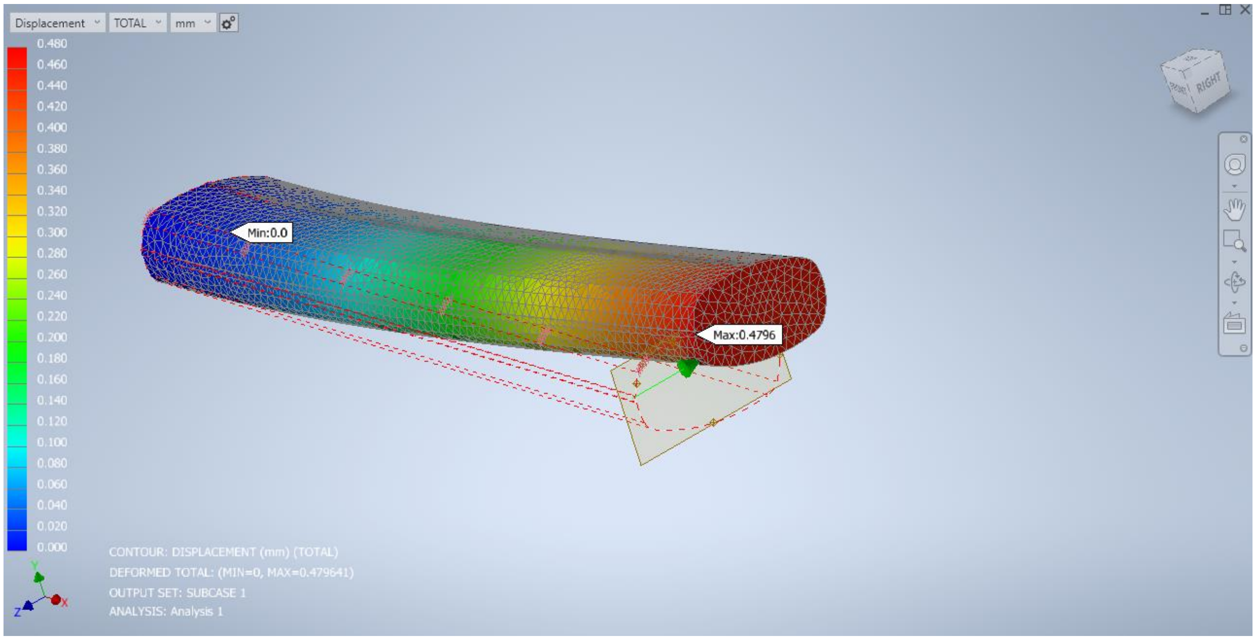

Figure 10.6: Vertical displacement of a beam.

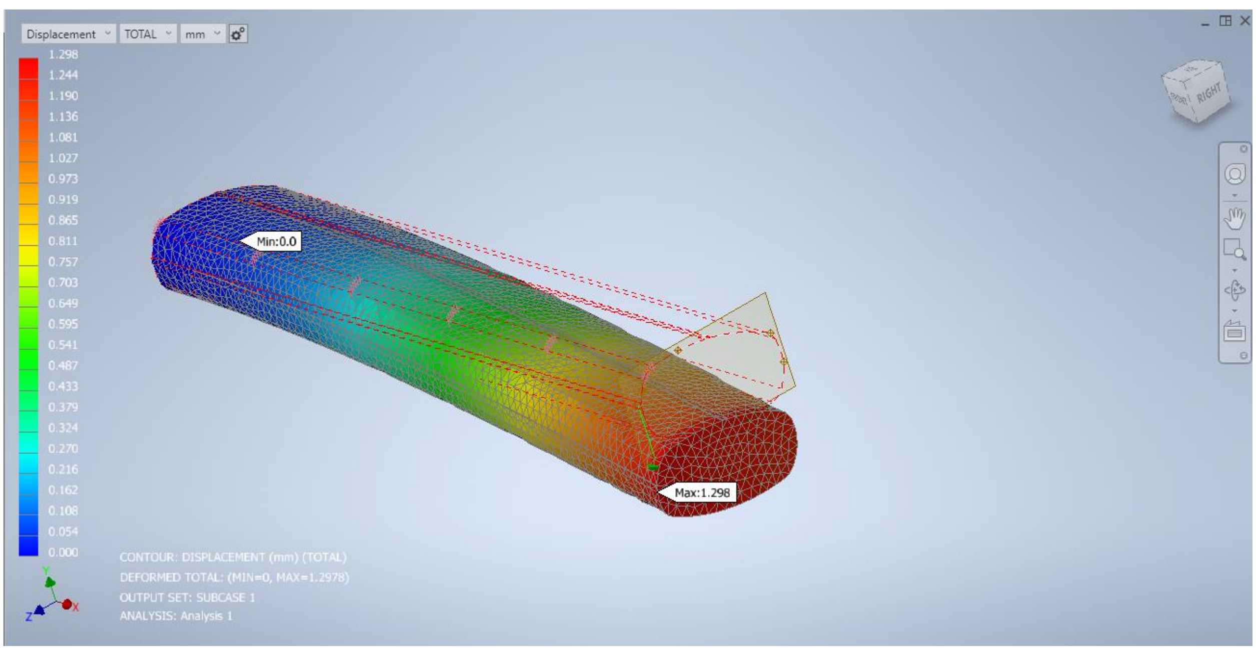

Figure 10.7: Axial displacement of a beam.

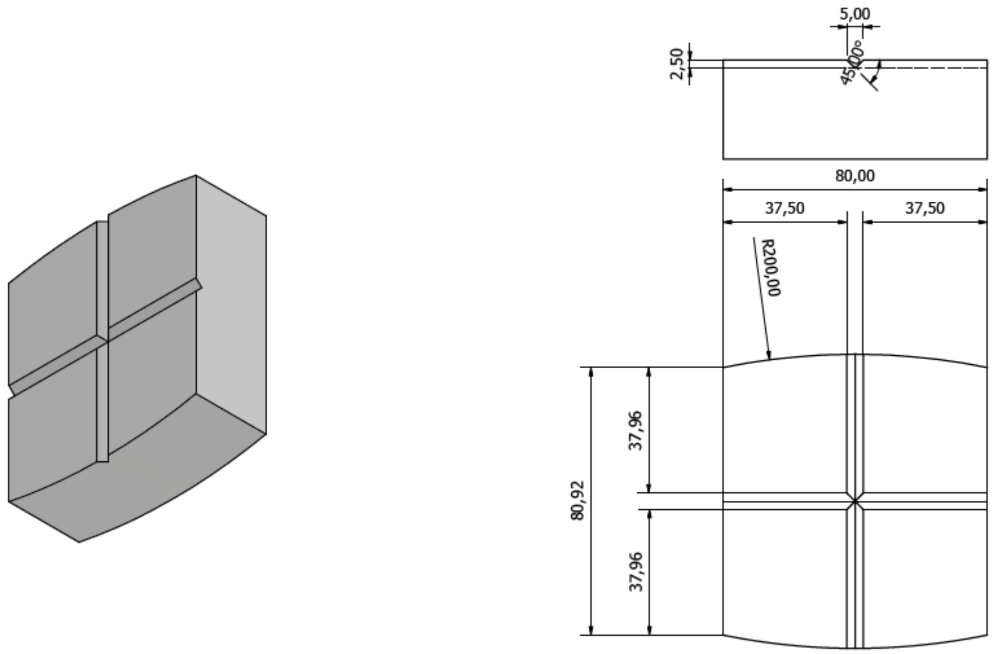

Figure 10.8: Mechanical drawing of the pass line's profile.

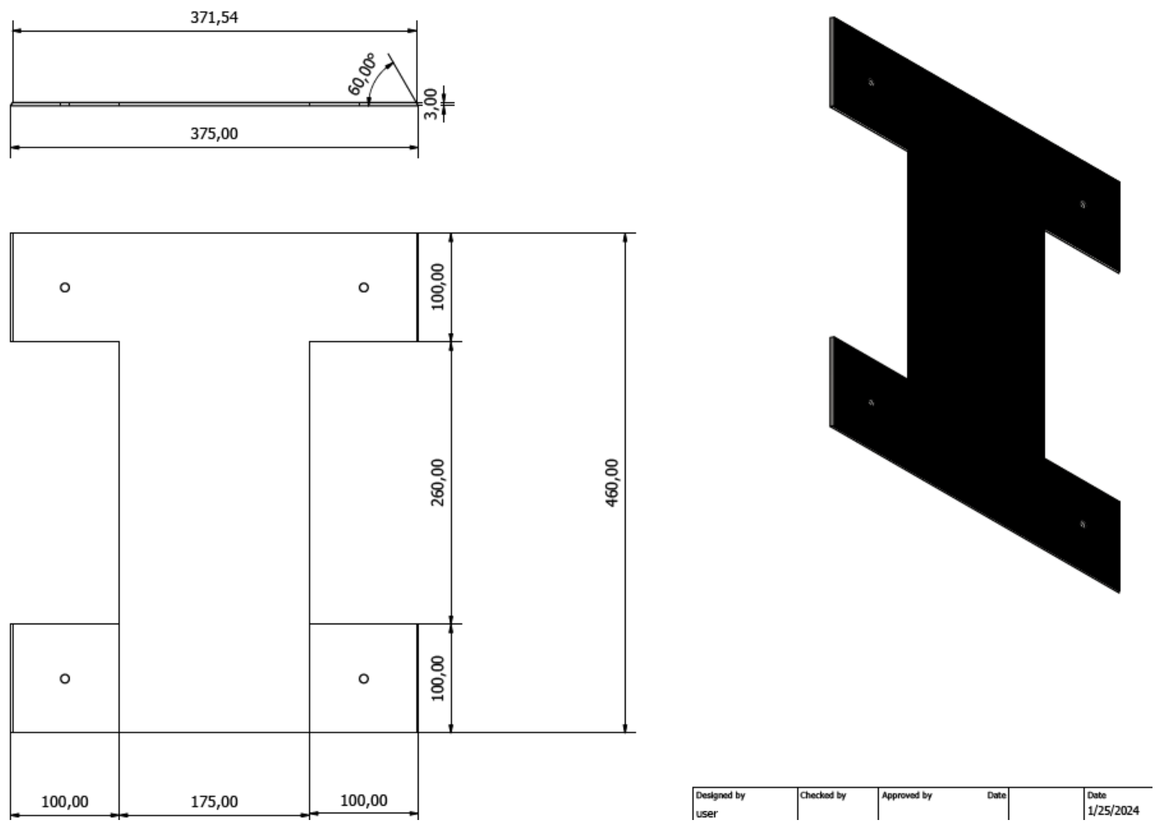

Figure 10.9: Mechanical drawing of the steel laminate.

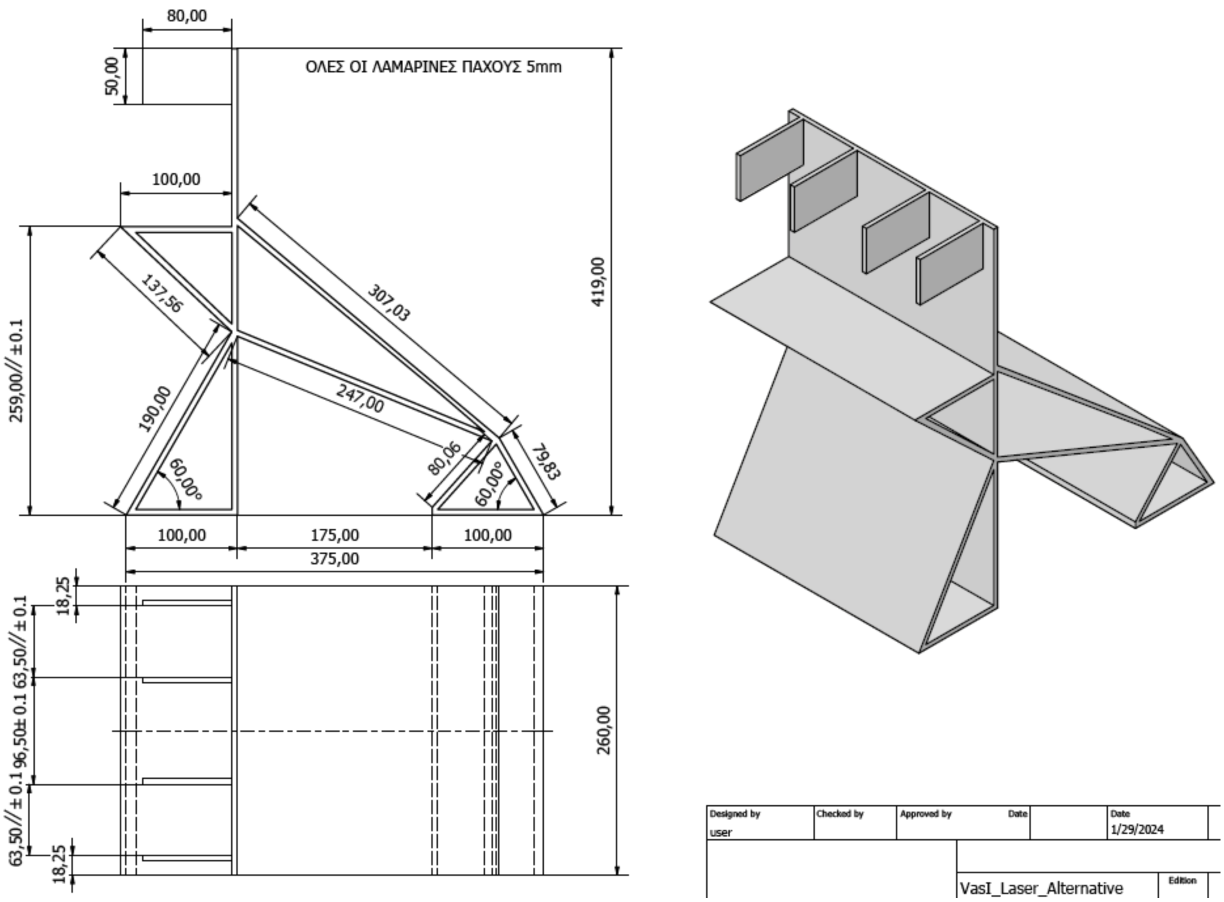

Figure 10.10: Mechanical drawing of the laser's base.

Figure 10.11: Alignment Laser.